DOI: 10.1002/ejic.201000839

Atmospheric Pressure Chemical Vapour Deposition of $TiCl_4$ and $tBuAsH_2$ to Form Titanium Arsenide Thin Films

Tegan Thomas,[a] Christopher S. Blackman,[a] Ivan P. Parkin,[a] and Claire J. Carmalt*[a]

Keywords: Titanium / Arsenic / Thin films / Chemical vapour deposition

Titanium arsenide thin films were deposited by the atmospheric-pressure chemical vapour deposition (APCVD) of $TiCl_4$ and $tBuAsH_2$ at substrate temperatures between 450 and 550 °C. The deposited films are typically silver in appearance, demonstrate good adherence and were identified by X-ray powder diffraction as crystalline TiAs. X-ray photoelectron spectroscopy (XPS) and Raman microscopy support the formation of TiAs. The TiAs films have an approximate 1:1 ratio of Ti:As, as identified by wavelength dispersive analysis of X-rays (WDX), and the films grow by an island growth mechanism with deposition rates of ca. 0.1 μm min^{-1}. The films display borderline metallic/semiconductor conductivity and those deposited at 550 °C possess high hardness.

Introduction

Thin films of early transition metal nitrides have received great interest due to their associated hardness and semiconductor properties. Titanium nitride is one such example, which, due to its hardness, chemical resistivity and attractive gold appearance, now finds commercial applications within the protective coatings of tools and machinery, along with decorative coatings.[1–3] Titanium nitride (TiN) thin films have been successfully deposited by atmospheric pressure (AP) and low pressure (LP) chemical vapour deposition (CVD) using both dual- (e.g. $TiCl_4/NH_3$) and single-source precursors, such as amido and imido titanium(IV) compounds.[4–7] Additionally, we have used silylamines and azides as precursors, which resulted in high quality TiN films,[8–10] and this methodology can be extended to other transition metal nitrides.[11] As the understanding of the roles of the precursor have developed, more user-friendly (i.e. safer and easier to handle) precursors have been introduced that have proved capable of not only depositing at much lower deposition temperatures, but also in producing high quality deposits.

In addition to metal nitrides, past research of phosphorus- and arsenic-containing thin films, namely the III/V semiconductors, has involved using PH_3 and AsH_3 for their deposition. Although these group 15 hydrides allowed relatively clean CVD reactions, alternatives were sought due to problems associated with toxicity, storage and handling. For example, substitution of PH_3 with isobutylphopshane or *tert*-butylphosphane ($tBuPH_2$), resulted in the successful deposition of InP epitaxial layers by the metal–organic vapour phase epitaxy reaction with trimethylindium. The deposited films were of high quality and comparable to those synthesised using PH_3.[12] Indeed, group 15 organoprecursors have demonstrated themselves as successful alternatives to the group 15 hydrides in the deposition of a variety of phosphorus compounds.[13] Recently we reported the first dual-source deposition of TiP films on glass substrates by the APCVD reaction of $TiCl_4$ with $tBuPH_2$,[14] from the reaction of $TiCl_4$ with a variety of primary phosphanes (RPH_2 where R = Ph, *t*Bu and Cy^{hex})[15] and from the reaction of $[Ti(NMe_2)_4]$ with $Cy^{hex}PH_2$.[16] Thereafter, we extended the methodology to deposit GeP using both primary and secondary phosphanes,[17,18] and also to deposit NbP,[19] TaP,[20] CrP,[21] MoP[22] and VP thin films.[23] In addition, SnP films have also been deposited using organophosphane alternatives to PH_3.[24]

Apart from CoAs,[25] MnAs,[26] and the key III/V materials (AlAs, GaAs and InAs), knowledge of metal arsenide thin film remains limited.[27] However, metal arsenides have been studied in their solid forms, where traditionally they have been formed by solid state metathesis reactions.[28–30] Following the previous results observed with the replacement of PH_3 by $tBuPH_2$,[12] similar studies were carried out to seek potential AsH_3 alternatives. GaAs films were successfully deposited by metal–organic (MO)CVD methods using $tBuAsH_2$, with the deposited films comparable in both quality and surface morphology to those previously achieved using AsH_3.[13,31] Therefore, utilising organoarsenic precursors for the deposition of transition metal arsenides was expected to result in the successful formation of metal arsenide films.

In this paper we report the formation of TiAs thin films on glass substrates by the APCVD reaction of $TiCl_4$ and $tBuAsH_2$ at substrate temperatures between 450 and

[a] Materials Chemistry Centre, Department of Chemistry, University College London,
20 Gordon St., London, WC1H 0AJ, United Kingdom
E-mail: c.j.carmalt@ucl.ac.uk

Supporting information for this article is available on the WWW under http://dx.doi.org/10.1002/ejic.201000839.

550 °C. The properties of the resulting films are compared with those previously reported for TiN and TiP thin films. Although some TiAs-like species were observed at the interface between GaAs and $SrTiO_3$ layers,[32] to the best of our knowledge this is the first formation of a TiAs thin film by a vapour deposition method (CVD or PVD).

Results and Discussion

The dual-source APCVD of $TiCl_4$ and tBuAsH_2 on to glass substrates was studied between 450–550 °C, using three different deposition times (Table 1). Below 450 °C no film was observed, however at 450 and 500 °C silver films were deposited and blue films were deposited with a gold appearance on the leading edge at 550 °C. All regions of the films, irrespective of colour, provide the same analytical results. A thickness gradient is observed moving along the film from the end nearest the precursor inlet (thickest); we therefore conclude that the different colours relate not to regions of different composition, but to regions of different thickness. Indeed, these blue and gold films are consistent with those previously reported on the leading edge of silver TiP films,[15] with both TiAs and TiP thin films different in visual appearance to metallic gold/purple thin films of TiN.[8] The films were highly reflective and did not show any changes in visual appearance after approximately one year's storage in air.

All films passed the Scotch-tape test, excluding the TiAs film deposited at 500 °C for 120 seconds which demonstrated areas of delamination. The blue TiAs film deposited at 550 °C was the only film to pass the steel stylus scratch test, indicating that these films are of comparable hardness to TiP.[15] Measurement of film resistivity showed that all films had resistivities in the range 10–50 mΩ cm, which is similar to that of TiP films,[15] and indicative of metallic- or semiconductor-like conductivity ($10–1 \times 10^{-6}$ Ω cm for metals and $10^{4}–10^{-3}$ Ω cm for semiconductors).[33] Measurement of reflectance and transmittance spectra showed that the thickest films (i.e. the 120 second deposits) exhibited 0% transmittance, whereas the thinnest films were partially transparent in the visible region (40% transmission) with approximately equal percentage transmittance over the wavelengths 300–2000 nm. All films demonstrated less reflectivity within the IR region. This is contrary to previously deposited TiP and TiN thin films which demonstrated an increased reflectivity within this region, and hence TiAs, unlike TiN and TiP, would not be suitable for use as a heat mirror.[8,15]

The TiAs films deposited at 450 °C and 550 °C using a deposition time of 120 seconds displayed water droplet contact angles of 45–60°, with a higher contact angle range of 70–90° observed at 500 °C. These values are typical of hydrophobic films and are in agreement with that previously reported for TiP thin films, which were similarly hydrophobic.[15]

The films were characterized by a range of techniques. Compositional analysis of the films was determined by WDX analysis, which showed that the films had variable titanium to arsenic ratios. However, for films deposited at 500 °C with a deposition time of 60 seconds or greater (mixing chamber temperature below 140 °C), this ratio was close to 1:1 with approximately 5 at.-% incorporation of chlorine within all deposited films. This chlorine incorporation is higher than observed for analogous TiP deposits, where chlorine incorporation was considered negligible.[15] It should be noted that in these previous studies the phosphane was in a 4:1 excess, whereas the arsine:$TiCl_4$ ratio in the present work was only 2:1. Subsequent experiments carried out with a 4:1 ratio of tBuAsH_2/$TiCl_4$ reduced chlorine contamination in the TiAs films to 1 at.-% or less. However, the molar flow of arsine is high under these conditions, and safety concerns regarding abatement of unreacted arsenic species meant that more extensive experiments were not performed under these conditions. Typically all silver and blue TiAs thin films demonstrated good substrate coverage, with the observation of more uniform films upon an increase in deposition time. Scanning electron microscopy (SEM) showed spherical regions on all films where material had failed to nucleate and deposit (Figure 1). To investigate the mechanism of the TiAs thin film deposition, comparative image analysis was conducted on films deposited at 500 °C using deposition times of 30, 60 and 120 seconds (consequently depositing films of varying thickness) (Figure 2, a–c). SEM showed that the TiAs films were made up of roughly spherical agglomerates of approximately 0.15, 0.2 and 0.4 μm depending upon the deposition time. The sequence of images as shown in Figure 2 illustrates the gradual build up of the particles into agglomerates to form thicker and more continuous films; these images show an island growth mechanism, which is consistent with previously reported TiP films.[15] In addition, SEM analysis was conducted on three TiAs films deposited

Table 1. Experimental conditions and resultant film compositions as determined by WDX analysis, for films deposited by the APCVD of $TiCl_4$ and tBuAsH_2.

Substrate Temp. [°C]	N_2 flow rate through $TiCl_4$ bubbler, L min^{-1}; (mol min^{-1})	N_2 flow rate through tBuAsH_2 bubbler, L min^{-1}; (mol min^{-1})	Plain line flow, [L min^{-1}]; mixing chamber; temp. [°C]	Deposition time [s]	WDX analysis	Film colour
450	0.18; (0.00066)	0.1; (0.00128)	4; 130	120	$TiAs_{0.74}$	silver
500	0.18; (0.00066)	0.1; (0.00128)	4; 135	120	$TiAs_{1.1}$	silver
550	0.18; (0.00066)	0.1; (0.00128)	4; 130	120	$TiAs_{0.72}$	deep blue
500	0.18; (0.00066)	0.1; (0.00128)	4; 140	30	$TiAs_{1.31}$	silver
500	0.18; (0.00066)	0.1; (0.00128)	4; 130	60	$TiAs_{0.96}$	silver
500	0.18; (0.00066)	0.2; (0.00257)	4; 140	120	$TiAs_{0.72}$	silver

using the same deposition time (120 seconds) but at different substrate temperatures (Figure 2, d–f). Increased substrate temperature resulted in increased film growth, which resulted in more continuous films.

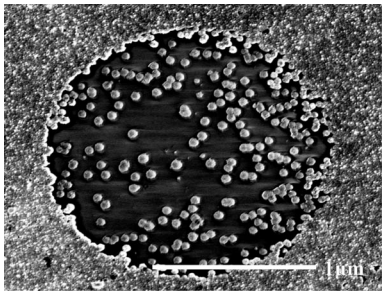

Figure 1. Scanning electron micrograph (at ×3,700) displaying an unnucleated area within the deposition of TiAs by the APCVD of $TiCl_4$ and tBuAsH_2 at 500 °C for 120 seconds.

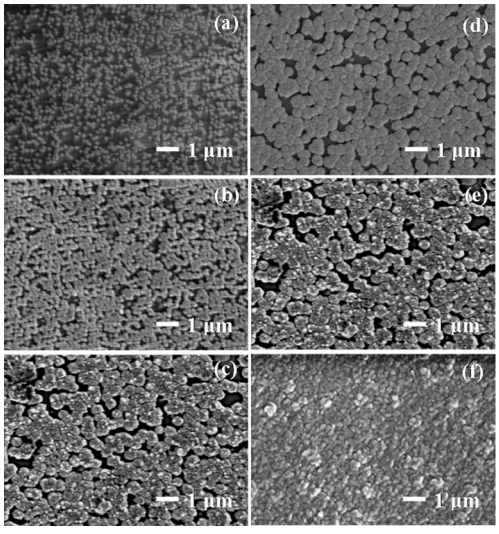

Figure 2. (a–c) Scanning electron micrographs (at ×10,000) of TiAs films deposited by the APCVD of $TiCl_4$ and tBuAsH_2 at 500 °C with deposition times of 30 (a), 60 (b), and 120 seconds (c). (d–f) Scanning electron micrographs (at ×10,000) of TiAs films deposited via the APCVD of $TiCl_4$ and tBuAsH_2 with a deposition time of 120 seconds and substrate temperatures of 450 (d), 500 (e) and 550 °C (f).

Film thickness for the films deposited at 120 seconds, determined using side-on SEM, increased with increasing temperature from approximately 190 nm at 450 °C to approximately 270 nm at 550 °C. Due to difficulties in obtaining an image for the film deposited at 500 °C for 120 seconds, a side-on SEM image for a TiAs film deposited at 500 °C for 60 seconds was obtained, which gave an approximate film thickness of 110 nm. Assuming a linear rate of deposition, this would lead to a film thickness of ca. 220 nm after 120 seconds. The deposition rates were therefore ca. 95 nm, 110 nm and 135 nm min^{-1} at substrate temperatures of 450, 500 and 550 °C, respectively. Assuming that $TiCl_4$ is the rate limiting reagent, the deposition rates of the TiAs films at 550 °C [200 µm min^{-1} mol $(TiCl_4)^{-1}$] are approximately half of those of TiP films deposited using tBuPH_2 at 550 °C [540 µm min^{-1} mol $(TiCl_4)^{-1}$].[15]

X-ray powder diffraction confirmed the silver and blue deposits as crystalline TiAs (Figure 3),[34] with strong peaks observed along the (102) and (110) planes, suggesting preferred orientation with the weakly diffracting (103) planes near-perpendicular to the scattering vector. TiAs is known to adopt the TiP structural type, where two nonequivalent phosphorus atoms occupy octahedral or trigonal prismatic holes, with a difference of 0.11 Å between the two Ti–P bond lengths.[35] The TiP and TiAs systems are different in structure to TiN, which adopts the NaCl rock-salt structure.[36] In addition to the TiAs peaks, the X-ray powder diffractogram showed a broad peak at approximately 22° which can be attributed to the underlying glass substrate. From line broadening studies an approximate crystal size of 0.09 µm was obtained.

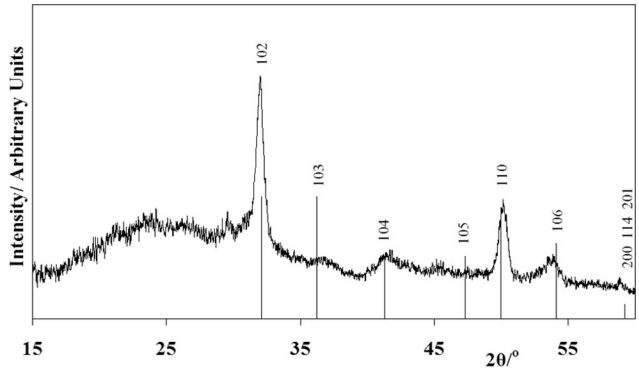

Figure 3. X-ray powder diffraction pattern of TiAs film deposited by the APCVD of $TiCl_4$ and tBuAsH_2 at 500 °C, with comparison to a reference TiAs diffractogram.[34]

XPS analysis of a TiAs film deposited at 500 °C showed that a variety of Ti $2p_{3/2}$ and As $3d_{5/2}$ environments were present at the surface. The surface Ti $2p_{3/2}$ ionisation displayed one principal environment at 458.5 eV which is assigned as TiO_2,[37] and two minor environments at 454.0 and 456.5 eV. The As $3d_{5/2}$ ionisation showed two environments centred on 40.0 and 40.9 eV. The peak at 40.0 eV is assigned to the formation of TiAs, in agreement with other metal arsenides,[37] and this corresponds to the Ti $2p_{3/2}$ ionisation at 454.0 eV, consistent with the observed 1:1 ratio for the normalised peak areas, with a similar Ti $2p_{3/2}$ ionisation observed for TiP.[38] The remaining unassigned ionisations were those of Ti $2p_{3/2}$ at 456.5 eV, As $3d_{5/2}$ at 40.9 eV and O 2p at 535.4 eV; these may relate to a titanium arsenic oxygen species [such as $Ti_3(AsO_4)_4$], however, no literature data is available and the binding energies are at the extremes of the normal range for each of the elements. Upon etching the film, the peaks attributed to the titanium arsenic oxygen species are rapidly reduced to below the detection level of the technique. Thus, the depth profile indicates the three peaks are linked but due to their positions we were unable to assign them to any known species. The formation of elemental arsenic was discounted be-

cause, if this resulted from precursor decomposition, we would expect arsenic to be present throughout the material and not simply segregated at the surface and the Ti and O ionisations would not be expected to decrease at an identical rate. The ionisations associated with TiO_2 also decreased dramatically with etching, with TiO_2 contributing to approximately 70% of the titanium species at the surface, with reduction to approximately 20% within the bulk, indicating that an oxidised overlayer is present; this finding is identical to our previous findings for TiP.[15] The formation of the surface limited oxide species is therefore ascribed to oxidation occurring after the CVD process, i.e. on exposure to atmospheric conditions. After approximately one year of storage in air, WDX analysis was repeated on the TiAs film deposited at 500 °C for 120 seconds. The oxygen content was found to be consistent with that first reported for the film supporting this conclusion.

Raman microscopy was conducted on all of the TiAs films. The Raman patterns were virtually identical at all points along the glass and were consistent for films deposited at different substrate temperatures. Comparison of the Raman patterns obtained at 500 °C using three different deposition times (30, 60 and 120 seconds) showed that all three patterns display consistent bands (Figure 4); two relatively intense sharp peaks at 193 and 244 cm^{-1}, and two weak broad peaks at 420 and 600 cm^{-1}. Comparison with the Raman spectrum of TiP, which exhibits two main peaks at 320 and 248 cm^{-1},[15] shows that the spectra appear to be consistent with the two main TiAs peaks appearing at lower energies as expected for substitution of the lighter P atom for the heavier As atom in the crystal structure.

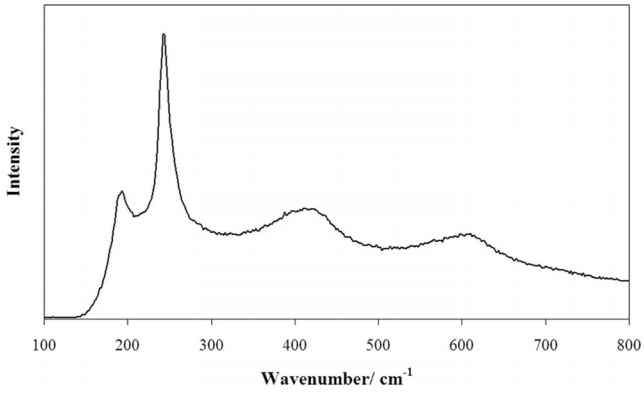

Figure 4. Raman spectra for a TiAs film deposited by the APCVD of $TiCl_4$ and tBuAsH_2 at 500 °C for 120 seconds.

AFM was conducted on three TiAs films formed using a deposition time of 120 seconds, and substrate temperatures of 450, 500 and 550 °C. Visible differences between the films were observed between the AFM images (Figure 5). At the lower temperature of 450 °C, the TiAs film exhibits the highest roughness with an RMS value of 44.9 nm. As the temperature is increased to 500 °C, the surface roughness decreased to 21.3 nm and at 550 °C to 20.2 nm. This is consistent with the SEM images shown in Figure 2 which show more isolated island deposits at lower deposition temperatures, contributing to the increased surface roughness.

The mechanism for the deposition of TiAs from $TiCl_4$ and tBuAsH_2 from APCVD was not investigated in this study. The deposition of TiAs films worked best at substrate temperatures of 500 °C and films were not deposited below 450 °C. These results suggest that temperatures in excess of 450 °C are required for the precursors to react completely and form a film. If excess arsine is employed the chlorine contamination in the resulting films is low (< 1 at.-%), despite the use of $TiCl_4$, which indicates that a clean decomposition pathway is available. Previous calculations have shown that tBuAsH_2 decomposes through the loss of H_2 to give tBuAs, which, in turn, decomposes by β-H abstraction to form 2-methylpropene and AsH.[39] It is possible that this occurs during the APCVD reaction of $TiCl_4$ and tBuAsH_2, allowing a clean decomposition pathway. However, we have previously reported the reaction of $TiCl_4$ with a range of arsines, including tBuAsH_2.[40] In this study it was found that $TiCl_4$ forms 1:1 adducts with organoarsines, such as tBuAsH_2. Thus, it is possible that the APCVD reaction proceeds through the formation of gas phase adducts, for example [$TiCl_4$(tBuAsH_2)]. Further studies into the reaction chemistry are required in order to obtain a more definite mechanism for the APCVD reaction.

Conclusions

The APCVD of $TiCl_4$ and tBuAsH_2 at 500 °C with deposition times of 60–120 seconds successfully results in the deposition of titanium arsenide thin films by an island growth mechanism, with deposition rates of ca. 100 nm min^{-1}. The titanium arsenide thin films are typically silver in appearance, exhibit good adherence and demonstrate regions of blue and gold deposits upon an increase in

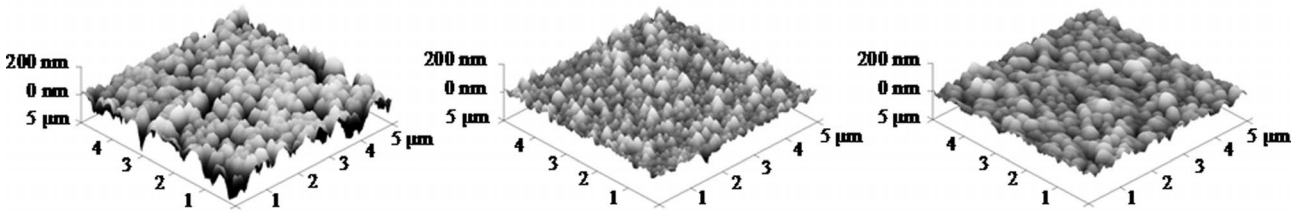

Figure 5. Atomic force micrographs of TiAs deposited by the APCVD of $TiCl_4$ and tBuAsH_2 at 450, 500 and 550 °C (left to right), with a deposition time of 120 seconds; micrographs represent a 5 µm × 5 µm region.

substrate temperature. The films exhibit an approximate 1:1 ratio of Ti:As, in addition to a 5 at.-% chlorine incorporation. Increasing the arsane:$TiCl_4$ ratio significantly reduces the chlorine incorporation. The films are electronically conductive, hydrophobic and optically transparent when sufficiently thin. Films deposited at 450 and 550 °C are typically arsenic-deficient which is attributed to surface oxidation.

Experimental Section

Caution! *It should be noted that the use of $tBuAsH_2$ could produce AsH_3 which is highly toxic. All the experiments were conducted in a fume cupboard, with the gas from the CVD process treated with bleach to destroy possible AsH_3.*

Chemical Vapour Deposition: Depositions were conducted on 90 mm × 45 mm × 4 mm SiCO float-glass supplied by Pilkington. Substrates were cleaned using petroleum ether (60–80 °C) and 2-propanol and allowed to air dry prior to use. All experiments were conducted using a horizontal cold wall APCVD reactor, comprising a graphite heating block containing a Watlow cartridge heater, with temperature control achieved using a Pt-Rh thermocouple. All APCVD equipment, parameters and methodology used were identical to that previously reported.[15] Deposition times varied between 30 and 120 seconds. Exact flows, temperatures and deposition times used during experiments are shown in Table 1. Upon deposition completion, the CVD chamber and substrate were allowed to cool to room temperature under a flow of nitrogen, before extraction of the substrate plus deposit, which were subsequently stored in air.

Titanium(IV) chloride (99.9%, Sigma Aldrich) (used as supplied without further purification) was placed in a stainless-steel bubbler, which was fitted with a heating jacket set to 60 °C in all instances. Redirection of hot gas flow into the bubbler introduced $TiCl_4$ into the flow system. tBuAsH_2 (SAFC Hitech Ltd.) (used as supplied without further purification) was used at room temperature, with the redirection of hot gas flow into the bubbler, resulting in tBuAsH_2 introduction into the flow system.

Film Analysis: X-ray powder diffraction patterns were obtained with a Bruker AXS D8 discover machine using monochromatic Cu-K_α radiation. WDX analysis was performed with a Philips XL30ESEM machine. High resolution X-ray photoemission spectra were recorded with a Kratos Axis Ultra DLD spectrometer at the University of Nottingham, using a monochromated Al-K_α (hv = 1486.6 eV) X-ray source. A standard wide scan with high resolution large areas (ca. 300 × 700 microns) with pass energies of 80 and 20 were used, respectively. The photoelectrons were detected using a hemispherical analyzer with channelplates and Delay line detector. The etch was performed using 4 keV Argon ions, using a Kratos minibeam III, rastered over an approximate area of 0.7 cm with an approximate etch rate of 6 Å min^{-1}. The binding energies were referenced to an adventitious C 1s peak at 284.9 eV. Raman spectra were acquired with a Renishaw Raman system 1000, using a helium/neon laser of wavelength 632.8 nm. The Raman system was calibrated against the emission lines of neon. SEM was conducted using a JSM-6301F scanning field emission machine. AFM was conducted with a Dimension 3100 AFM under ambient conditions. Reflectance and transmission spectra were recorded between 300 and 2500 nm using a Perkin–Elmer lambda 950 photospectrometer. Measurements were standardized relative to a spectralab standard mirror (reflectance) and air (transmission). Water contact angle measurements were conducted by measuring the spread of a 10 μL drop of water and applying an appropriate calculation.

Supporting Information (see also the footnote on the first page of this article): Side-on SEM, depth-profile XPS and Raman spectra.

Acknowledgments

The Engineering and Physical Sciences Research Council (EPSRC) is thanked for studentships (to T. T.) and a grant (EP/F019750/1) to Dr Emily Smith (University of Nottingham) who is thanked for carrying out XPS analysis (A Coordinated Open-Access Centre for Comprehensive Materials Analysis). Pilkington is thanked for providing the glass substrates and SAFC Hitech Ltd. is thanked for the supply of tBuAsH_2. I. P. P. thanks the Wolfson Trust/Royal Society for a merit award. Thanks goes to Prof. F. Cacialli and Mr Y. S. Shin (London Centre for Nanotechnology) for the AFM images, Dr R. Binions for help with UV/Vis and Drs S. Firth and G. Hyett for discussions about Raman and X-ray powder diffraction, respectively.

[1] J. Takadoum, H. H. Bennani, M. Allouard, *Surf. Coat. Technol.* **1997**, *88*, 232–238.
[2] J. P. Dekker, P. J. Vanderput, H. J. Veringa, J. Schoonman, *J. Electrochem. Soc.* **1994**, *141*, 787–795.
[3] S. R. Kurtz, R. G. Gordon, *Thin Solid Films* **1986**, *140*, 277–290.
[4] R. Fix, R. G. Gordon, D. M. Hoffman, *Chem. Mater.* **1991**, *3*, 1138–1148.
[5] R. M. Fix, R. G. Gordon, D. M. Hoffman, *Chem. Mater.* **1990**, *2*, 235–241.
[6] C. J. Carmalt, A. C. Newport, I. P. Parkin, A. J. P. White, D. J. Williams, *J. Chem. Soc., Dalton Trans.* **2002**, 4055–4059.
[7] C. J. Carmalt, A. Newport, I. P. Parkin, P. Mountford, A. J. Sealey, S. R. Dubberley, *J. Mater. Chem.* **2003**, *13*, 84–87.
[8] A. Newport, C. J. Carmalt, I. P. Parkin, S. A. O'Neill, *J. Mater. Chem.* **2002**, *12*, 1906–1909.
[9] C. J. Carmalt, S. R. Whaley, P. S. Lall, A. H. Cowley, R. A. Jones, B. G. McBurnett, J. G. Ekerdt, *J. Chem. Soc., Dalton Trans.* **1998**, 553–557.
[10] C. J. Carmalt, A. H. Cowley, R. D. Culp, R. A. Jones, Y. M. Sun, B. Fitts, S. Whaley, H. W. Roesky, *Inorg. Chem.* **1997**, *36*, 3108–3112.
[11] S. E. Potts, C. J. Carmalt, C. S. Blackman, F. Abou-Chahine, D. Pugh, H. O. Davies, *Organometallics* **2009**, *28*, 1838–1844.
[12] C. H. Chen, C. A. Larsen, G. B. Stringfellow, D. W. Brown, A. J. Robertson, *J. Cryst. Growth* **1986**, *77*, 11–18.
[13] C. J. Carmalt, S. Basharat, in: *Precursors to Semiconducting Materials*, in: *Comprehensive Organometallic Chemistry*, D. O'Hare, Elsevier Ltd., Oxford, UK, **2007**, vol. 12.
[14] C. Blackman, C. J. Carmalt, S. A. O'Neill, I. P. Parkin, L. Apostilco, K. C. Molloy, *J. Mater. Chem.* **2001**, *11*, 2408–2409.
[15] C. Blackman, C. J. Carmalt, I. P. Parkin, S. O'Neill, L. Apostolico, K. C. Molloy, S. Rushworth, *Chem. Mater.* **2002**, *14*, 3167–3173.
[16] C. S. Blackman, C. J. Carmalt, S. A. O'Neill, I. P. Parkin, L. Apostolico, K. C. Molloy, *Chem. Mater.* **2004**, *16*, 1120–1125.
[17] L. Apostolico, M. F. Mahon, K. C. Molloy, R. Binions, C. S. Blackman, C. J. Carmalt, I. P. Parkin, *Dalton Trans.* **2004**, 470–475.
[18] R. Binions, C. J. Carmalt, I. P. Parkin, *Polyhedron* **2003**, *22*, 1683–1688.
[19] C. S. Blackman, C. J. Carmalt, S. A. O'Neill, I. P. Parkin, K. C. Molloy, L. Apostolico, *J. Mater. Chem.* **2003**, *13*, 1930–1935.
[20] C. S. Blackman, C. J. Carmalt, I. P. Parkin, S. A. O'Neill, K. C. Molloy, L. Apostolico, *Mater. Lett.* **2003**, *57*, 2634–2636.
[21] C. S. Blackman, C. J. Carmalt, T. D. Manning, I. P. Parkin, L. Apostolico, K. C. Molloy, *Appl. Surf. Sci.* **2004**, *233*, 24–28.

[22] C. S. Blackman, C. J. Carmalt, T. D. Manning, S. A. O'Neill, I. P. Parkin, L. Apostolico, K. C. Molloy, *Chem. Vap. Deposition* **2003**, *9*, 10–13.
[23] C. S. Blackman, C. J. Carmalt, S. A. O'Neill, I. P. Parkin, K. C. Molloy, L. Apostolico, *Chem. Vap. Deposition* **2004**, *10*, 253–255.
[24] R. Binions, C. S. Blackman, C. J. Carmalt, S. A. O'Neill, I. P. Parkin, K. Molloy, L. Apostilco, *Polyhedron* **2002**, *21*, 1943–1947.
[25] Y. Senzaki, W. L. Gladfelter, *Polyhedron* **1994**, *13*, 1159–1167.
[26] P. A. Lane, B. Cockayne, P. J. Wright, P. E. Oliver, M. E. G. Tilsley, N. A. Smith, I. R. Harris, *J. Cryst. Growth* **1994**, *143*, 237–242.
[27] M. F. Mahon, N. L. Moldovan, K. C. Molloy, A. Muresan, I. Silaghi-Dumitrescu, L. Silaghi-Dumitrescu, *Dalton Trans.* **2004**, 4017–4021.
[28] A. L. Hector, I. P. Parkin, *Z. Naturforsch. Teil B: Chem. Sci.* **1994**, *49*, 477–482.
[29] A. L. Hector, I. P. Parkin, *J. Mater. Chem.* **1994**, *4*, 279–283.
[30] I. P. Parkin, *Chem. Soc. Rev.* **1996**, *25*, 199–207.
[31] R. M. Lum, J. K. Klingert, M. G. Lamont, *Appl. Phys. Lett.* **1987**, *50*, 284–286.
[32] Y. Liang, J. Kulik, T. C. Eschrich, R. Droopad, Z. Yu, P. Maniar, *Appl. Phys. Lett.* **2004**, *85*, 1217–1219.
[33] A. R. West, *Basic Solid State Chemistry*, 3rd ed., Wiley, **1999**.
[34] K. Bachmayer, H. N. Nowotny, A. Kohl, *Monatsh. Chem.* **1955**, *86*, 39–43.
[35] P. O. Snell, *Acta Chem. Scand.* **1967**, *21*, 1773–1776.
[36] R. A. Fischer, H. Parala, in: *Metal-organic Chemical Vapour Deposition of Refractory Transition Metal Nitrides*, in: *Chemical Vapour Deposition Precursors, Processes and Applications* (Eds.: A. C. Jones, M. L. Hitchman), Royal Society of Chemistry, Cambridge, UK, **2009**.
[37] C. D. Wagner, J. F. Moulder, L. E. Davis, W. M. Riggs, in: *Handbook of X-ray Photoelectron Spectroscopy* (Ed.: G. E. Muilenberger), Perkin–Elmer, Eden Prairie, Minn, **1977**.
[38] C. E. Myers, H. F. Franzen, J. W. Anderegg, *Inorg. Chem.* **1985**, *24*, 1822–1824.
[39] D. F. Foster, C. Glidewell, G. R. Woolley, D. J. Colehamilton, *J. Electron. Mater.* **1995**, *24*, 1731–1738.
[40] T. Thomas, D. Pugh, I. P. Parkin, C. J. Carmalt, *Dalton Trans.* **2010**, *39*, 5325–5331.

Received: August 4, 2010
Published Online: November 4, 2010

